

EXPERIMENTAL MODAL ANALYSIS OF A PALM TREE LOG UNDER RADIAL VIBRATIONAL EXCITATION¹

*Djamel Ouis**

Associate Professor
of Architectural Engineering
King Fahd University of Petroleum & Minerals
Dhahran, Saudi Arabia
E-mail: djamel@kfupm.edu.sa

(Received June 2021)

Abstract. Trees may be subject to rot-inducing agents that degrade the strength of the material making their trunk, and decrease the quality of their crop. Several techniques, both nondestructive and destructive, are available for assessing the extent of damage caused by rot in a tree trunk. The present work presents the results of a preliminary study conducted on a palm tree trunk for isolating a specific mode from its response to a vibrational excitation, namely the so-called “ovalling” mode. The latter is cross-sectional and in a circular cylinder, and manifests itself relatively locally, ie has little dependence on the lateral extension of the cylinder. An experimental modal analysis is made on a piece of a date palm tree trunk when set into vibration through a radial mechanical excitation, and the response is collected at points along a circumference on the trunk. The value of the resonance frequency of the ovalling mode was found to be somehow variable, probably resulting from some coupling phenomena between various modes of vibration due to the inhomogeneity, anisotropy, and fiber-like structure of the trunk wood. As rot usually affects markedly the strength of the trunk wood, the frequency of the ovalling mode, which depends on the strength of the material, can be used for estimating the severity of rot attack in the trunk. A numerical simulation is also made to a cylinder as a simplified representation of a tree trunk.

Keywords: Palm tree, modal analysis, vibration, cross-sectional mode, rot detection, nondestructive testing.

INTRODUCTION

In countries with hot climate, palm trees are an important part of the landscape. Date palm trees in the hot Middle Eastern areas, as well as oil and coconut palm trees in the more temperate and humid climates by the Equator tropic are also important sources of revenue for their fruit or the oil extracted from them. Trees in general are vulnerable to attack by pests that weaken the trunk after some time of activity in it. Rot-infected trees standing in city parks and streets may constitute potential hazards to passersby, and the trees in plantations require constant control of their health status. The reliance on a fast and efficient monitoring procedure becomes therefore necessary to decide on the felling and clearing of a tree from the site. The use of the technique, if successful, will not be restricted to use in palm trees, but will

encompass any kind of trees while standing, or to logs and wooden utility poles.

The present study has for its main goal to investigate the health condition of a tree trunk through simply striking it by a hammer blow and then recording and analyzing the response to that excitation. The nondestructive technique that will be developed for date palm trees is expected to cover other tree species as well. Hence once the vibrational behavior of the tree stem is known, and the resonant mode of vibration of interest identified, along with its frequency for each tree species, it is possible to establish a “soundness chart” for determining the extent of rot attack in the stem. Such a chart expresses the proper frequency of the vibration mode as a function of the geometrical characteristics of the stem, such as its width and length.

REVIEW OF LITERATURE ON TREES

Rot attacks almost all tree species and often spreads from the roots up to the trunk of the tree.

* Corresponding author

¹ The copyright of this article is retained by the authors.

It is the result of attack by certain species of fungi, and the consequent colonization of the tree stem leads to decay by which the mass of the wood is reduced and its strength is weakened. Visual inspection of the tree, core sample-taking from the trunk, and the measurement of resistance to drill are a few of the commonly accepted methods used in forestry and urban trees' inspection for the detection of decay in trees. The former is rather based on subjective interpretation of external signs, which often makes it an unreliable method (Wagener and Davidson 1954). The second method, which consists of taking core samples from the tree trunk by means of an increment borer, is also found to be somehow unreliable in predicting the percentage of decayed trees in a forest stand. Its unreliability becomes even more accentuated when the location of rot is off the pith, the center axis of the trunk, and in which case hitting a decayed area becomes less likely when taking the core sample. Moreover, it has been found that the success in finding decay is lower when the core sample is taken at breast height than at a lower height near ground level (Stenlid and Wåsterlund 1986). A tree may live with the wounds caused by the increment borer; the destructive nature of the method may increase the susceptibility to rot.

Nondestructive detection methods are based on various different technologies and have been suggested during the last few decades. Many of these methods are based on acoustical techniques and function on scanning the interior cross section of the tree trunk through setting it to an impulse excitation and then establishing an image through processing the data collected from an array of sensors attached to the surface of the tree trunk (Rust 2000; Deflorio et al 2008). This is a more elaborate way of implementing earlier and simpler vibrational techniques where a single sensor is used for measuring the time of flight of the mechanical pulse induced in the tree trunk. A stress wave is thus generated by, for instance, a hammer strike, and calculations of the speed of wave propagation permits to determine the stiffness of the material as expressed in terms of the Modulus of Elasticity, MOE (wood is a highly

anisotropic material, and more specifically a tree trunk exhibits radial anisotropy, and the determination of the strength properties of the material is highly dependent on the direction of wave propagation within the material). The extent of the zone of rot attack and the degree of its severity in the tree trunk may be established through comparing the measured speed of wave propagation, or the MOE, depending on to what extent the values of these parameters fall below a species-dependent threshold (Matthcek and Bethge 1993).

In this work, the modes of vibration of a piece cut transversally from the trunk of a date palm tree are investigated. The purpose of this preliminary investigation is to list the few lowest modes of vibration, both in shape and frequency, when a tree trunk is excited by a radial excitation. The study, which is of a pilot character, is limited to the few lowest vibration modes for the sole reason that these are the most important ones when it comes to examine the response of a tree trunk to mechanical excitation. Moreover, as a tree trunk behaves as a complex mechanical system (because of the various kinds of modes that the trunk may exhibit in its response to a mechanical excitation), and the response of modes is most pronounced for the lowest ones and tends to decrease for modes of higher order. For instance, it is known from studies carried on wooden beams that rot, as well as other structural defects, reduce the stiffness of the material as quantified by the value of its MOE. As a consequence it is found that the frequency of resonance, or eigenfrequency, of the flexural modes is also diminished, however, without too appreciably affecting the shape of these bending modes (Yang et al 2002; Choi et al 2007).

MATERIALS AND METHODS

The purpose from the present experimental study is to conduct an investigation into the various vibrational modes of interest in a palm tree trunk. Hence, a log was cut from the trunk of a sound palm tree and is in the first set of experiments set upon thin supports at about the nodes of the first flexural mode of vibration. In the second set of experiments, the log is hinged with its axis in the

vertical direction, to study the characteristics of the circumferential expansion modes of vibrations. A broadband signal is then fed into a shaker attached to the middle of the log and the response of the log to the excitation is recorded by an accelerometer. This latter is displaced stepwise over the whole cylindrical area of the log. The frequency and vibrational shape of the excited mode are thus determined from the analysis of the frequency response of the log at each of the positions considered.

Materials

A series of measurements were conducted on a log that was cut from the trunk of a date palm tree. The experiments conducted on the log were divided into two series, one series being where the log was laid horizontally on two supports and the other series with the log maintained standing and held at its two ends by sharp metallic rods.

The palm log was almost cylindrical in shape as the flaring was negligible along its axial direction, 110 cm of length and with an average perimeter of 143 cm, making an average diameter of 45.5 cm. Prior to making measurements, the log was wrapped with a thin plastic film, on which were glued equidistant tape strips along the axis, and other equidistant strips on its circumference. The mesh thus obtained was composed of cells of square shape, with an average size of $14 \times 14 \text{ cm}^2$. The axial strips were lettered in order from A to P, starting from the uppermost position on the log and moving around it, while the circumferential ones were numbered from 1 to 11, starting from the uppermost edge surface of the log and moving toward the bottom. Pictures over the measurement setups are shown in Fig 1, with details over the vertical setup in Fig 2. An illustration of the vertical setup with the connections of the measurement equipment is also shown in Fig 3. The setup makes, in total, 176 measurement points, evenly distributed on the surface of the log and that will be used for mapping the vibration amplitude on the surface of the log.

Experimental Modal Analysis, EMA

Experimental Modal Analysis, EMA (or modal testing), has grown steadily in popularity since the advent of the digital Fast Fourier Transform, FFT, spectrum analysis technique in the mid-1970s. It has become a widely accepted tool that is used in structural engineering and material sciences for the nondestructive evaluation of mechanical properties of materials and structures. The principle of using EMA is built about setting a structure into vibration through submitting it to a short impact and then study the response of the structure for determining its proper, or natural, modes of vibration (Schwarz and Richardson 1999).

An essential concept in EMA is that of the Frequency Response Function, or Frequency Transfer Function, and the measurement of which helps isolating the natural dynamic properties of the mechanical structure under investigation. The latter is a complex function and determines the relationship, expressed as a function of frequency, between excitation and response (or input and output), between two points on the structure under study.

Experimental Setup

The measurements on the log for the purpose of its modal analysis were conducted in the standing position. For the log in the horizontal setup, it was laid on the supports so that the boundary conditions were intended to satisfy approximately those of the first bending mode, that is to say, that the log was set on two wedge-like supports at a distance of one-sixth of its length from either of its ends. These are the positions of the nodes of this specific mode, and setting the supports at these nodes does not affect the flexural deflections of the log. A Brüel and Kjær, B&K, electrodynamic mini-shaker, model 4810, was then coupled to a steel rod, also usually called *stinger* in modal analysis parlance, to be connected to the vibrating cone of the shaker. The stinger, oriented in the radial direction of the log, was in its turn attached to a metallic plate in its turn screwed onto the log at its midst.

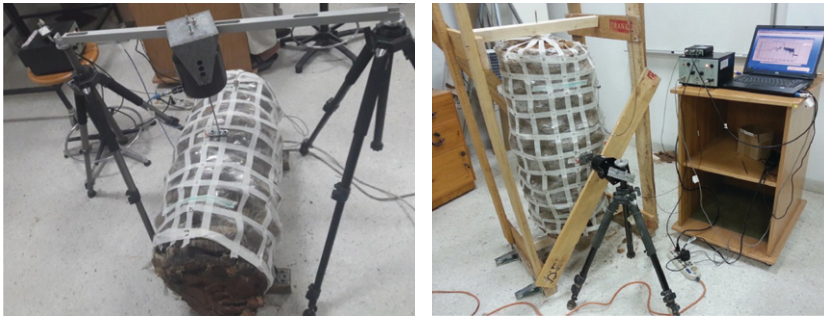


Figure 1. Pictures over the experimental measurement setup on the palm tree log. (a) Log on horizontal setup. (b) Log on vertical setup.

The vibration sensor consisted of a uniaxial piezoelectric charge accelerometer of type B&K 4381 with a sensitivity of 10 pC/ms^{-2} and a working frequency range from 0.1 Hz to 4800 Hz. To enable easy and fast displacement of the vibration sensor from a measurement position on the log to the next one, a needle-like screw 2.5 cm in length was attached to its base. The signal from the accelerometer was then fed into a B&K charge amplifier model B&K 2626 with the appropriate sensitivity calibration and signal amplification, and was maintained for the whole series of measurement positions so as to avoid inconvenient later adjustments of measurement data. This was accomplished through a prior reading of the response at a presumed position where the weakest response signal was expected to be recorded (at the most remote position on the log from the point of signal excitation, which is at the rim

of the log and diametrically opposed to the excitation position), and another reading at a measurement position where the signal was the most pronounced, ie nearest to the position of input of excitation signal. The charge amplifier was then set at a level with an acceptable signal-to-noise ratio at the weakest signal record, but at the same time without overloading the input to the amplifier at the position of the strongest signal. The measured signal was then conveyed to the input of a signal processor for the necessary cross-correlation operation to be executed with the signal that gave rise to it.

Measurement Technique

The quantity of interest that was measured is the impulse response, IR, which is acquired through submitting the test specimen to a chirp consisting



Figure 2. Pictures over details of the experimental measurement setup on the palm tree log. Left: Attachment of shaker, for force excitation. Right: Attachment of accelerometer, for response signal recording.

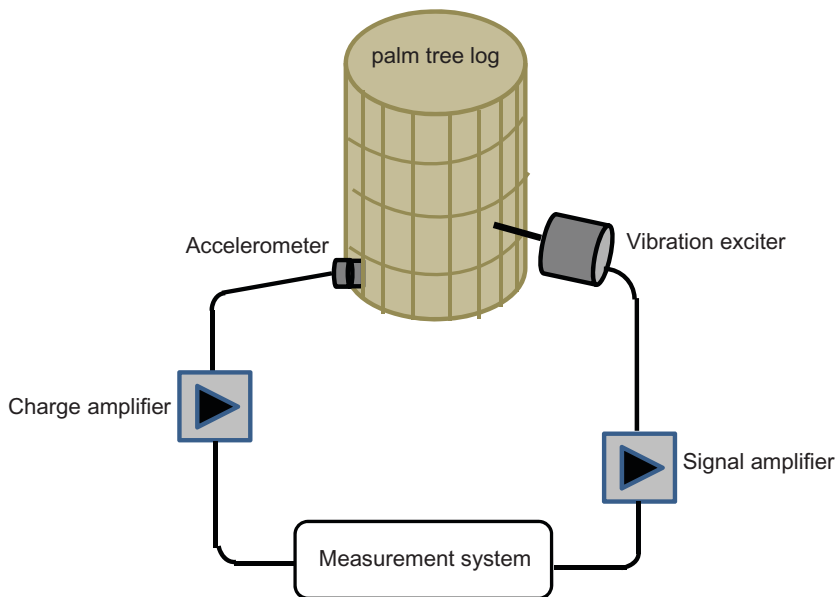


Figure 3. Schematic experimental set-up for measurements of the distribution of vibration amplitude on the log of the date palm tree set in vertical orientation.

of a sine sweep signal (this kind of excitation has shown superior reliability than the broadband random signal excitation, as it ensures, among others, higher immunity against distortion; Müller and Massarani 2001). In the actual measurement system the frequency sweep is set in the range 20–20,000 Hz and the sampling rate to 44,100 Hz prior to the FFT operation. For an FFT size of 8192 this gives a frequency resolution of 5.4 Hz for the frequency spectrum, or equivalently a time resolution of 0.19 s for the IR. The IR is thus obtained through executing a cross-correlation operation between the response recorded by the vibration sensor and the excitation signal. This measurement technique also spares the trouble of measuring the transfer function between the response signal and the excitation signal, and instead focuses on evaluating the FFT, of the impulse response at the measurement point.

A schematic representation over this measurement procedure is illustrated in Fig 4, and more details may be read in Kuttruff (2010). This measurement procedure has lately been incorporated

in the room-acoustical and simulation software ODEON software, which originally was designed for room acoustical simulations and calculations. For an appropriate level of the excitation signal above that of the background noise, and as the excitation signal is perfectly repeatable, the response result is also expected to be repeatable, hence avoiding the need for executing several measurements and then evaluating their average.

RESULTS

A typical signal trace of the IR, and its frequency counterpart, the transfer function, as recorded at measurement position P07 on the log are shown in Fig 5. The purpose from an antecedent measurement carried on the log on the horizontal mounting setup was to identify the approximate frequencies of the major natural vibration modes. This was conducted prior to the major measurement series at all measurement positions on the log. In the plot on the right-hand side of Fig 5, one can differentiate the peaks of some of the most important modes of vibration in the curve of

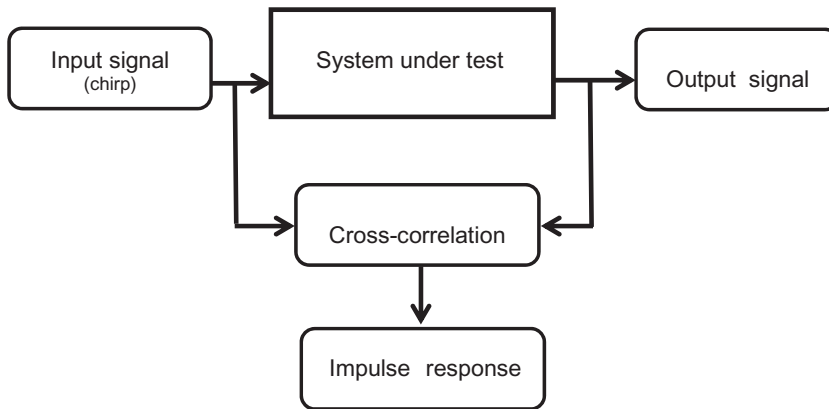


Figure 4. Illustration of the general principle behind the measurement procedure used for acquiring the impulse response of a system.

the amplitude as a function of the frequency. The first mode of vibration at around 45 Hz, depicted as “m,” is the mode of whole-body motion of the log, and which is at the resonance frequency of the spring-mass system composed of the log and the vibrating part of the shaker. The presence of this mode was made even more obvious when the log was set into vibration by the stronger shaker. The second mode, “b1,” in the range 180-210 Hz is the first bending mode, and the next one, “b2,” is the second bending mode with, theoretically, a frequency 2.55 that of the first bending mode, ie around 470 Hz. The next peak is that of the third bending mode, “b3,” with a frequency 5.44 that of the first one, ie around 900 Hz. It looks as if this mode vibrates at its most pronounced response at this measurement position, and its amplitude overrides that of the other two lower

bending modes. Next, the peak denoted as “o” on the frequency plot, has been investigated in the frequency responses of the measurement positions, and is found to be, to a high degree of confidence, the “ovalling” mode. However, its frequency is found to shift within the frequency range 1050-1600 Hz depending on the position of the sensor on the log. For some positions it did not exhibit lucid existence through a well-marked peak, like the one in Fig 5. More specifically, these positions of lesser display of the ovalling mode, were those positioned remotely far from the plane normal to the axis of action of the excitation signal, at a distance of approximately more than 30 cm along the axis of the log. An explanation of this position-dependent behavior of the modal amplitude and frequency of this cross-sectional mode is probably attributed to some

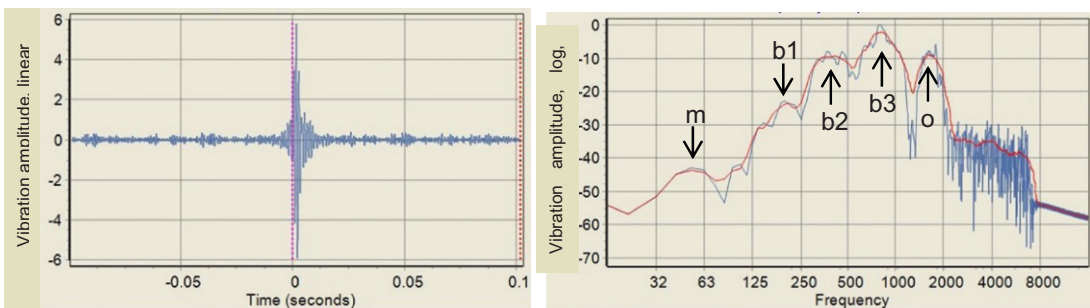


Figure 5. Left: Impulse response recorded at position P07 on the log. Right: Amplitude of the transfer function, ie the transform of the impulse response in the frequency domain.

coupling between this mode and the bending ones, and where a substantial part of the vibratory energy may be exchanged between the modes. The best performance of the ovaling mode was found on the circumference normal to the trunk's axis and containing the point of application of the excitation force. The manifestation of this mode showed a higher dampening of the vibration amplitude the farther away from the position of the excitation. The most plausible explanation to this behavior may be attributed to the inner fibrous structure of the trunk favoring the absorption of propagating vibratory energy through friction between contiguously packed fibers, which is believed to increase with increasing moisture content. Figure 6 depicts the linear vibration amplitude as recorded on the surface of the log on this circumferential line (measurements at positions 14 and 26 were not possible, hence unreliable, due to their falling in a deep trough, and the values of the vibration amplitude on the graph were simply extrapolated from those of positions on either of their sides). Polar plots, on both a linear and a logarithmic scale, are presented in Figure 7. The attenuation of the vibration amplitude of the ovaling mode, as depending on the lateral distance from the plane of application of the excitation signal, is illustrated in the curve plot of Fig 8. The measurement positions were taken on the line parallel to the axis of the log at 90° from the

excitation position and on either side of the plane of its application. At a distance about 30 cm from the plane of application of the excitation force, where the amplitude of vibration is maximum, the ovaling mode was scarcely observable. Its vibration amplitude was over 30 dB lower, ie less than ca. one-thirtieth of its highest value at the point of vibration excitation.

The graph in Fig 9 is a plot of the amplitude of vibration along a circumference of the log for the first bending mode at the frequency range between 180 Hz and 210 Hz, where it is seen the weak response on the lateral positions of the log. Measurements were conducted on the palm trunk at a lateral position mid-distance from the middle of the trunk toward its edge. Figure 10 presents polar plots of the amplitude of this first bending mode of vibration.

DISCUSSION

The modes of vibration that can be set into motion in the palm tree log may have various characters, and these can be arranged into the bending, cross-sectional, torsional, and longitudinal classes. Knowledge of the behavior, shape, and frequency of these modes will serve as a benchmark for a subsequent study concerned with establishing the degree of influence of rot on the physical and geometrical attributes of these

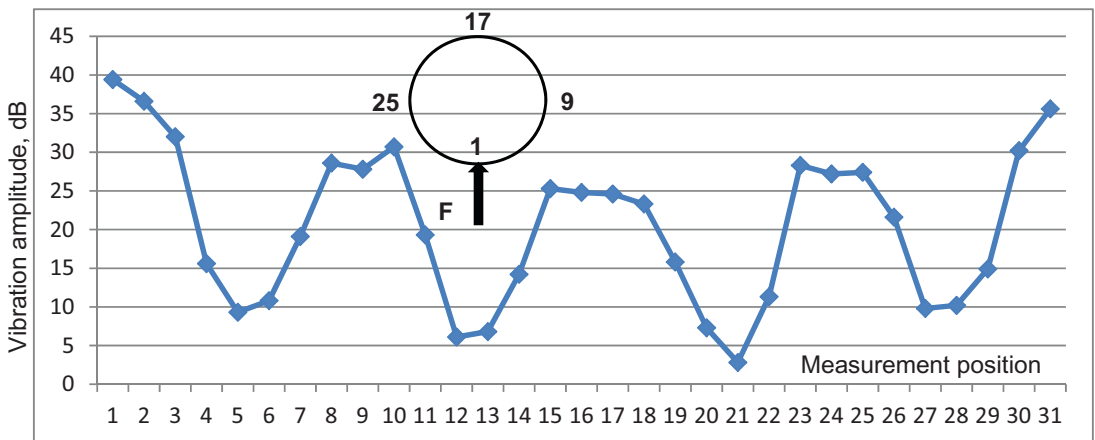


Figure 6. Vibration pattern along a circumference on the log for ovaling mode "o" at average frequency 1300 Hz. Linear amplitude.

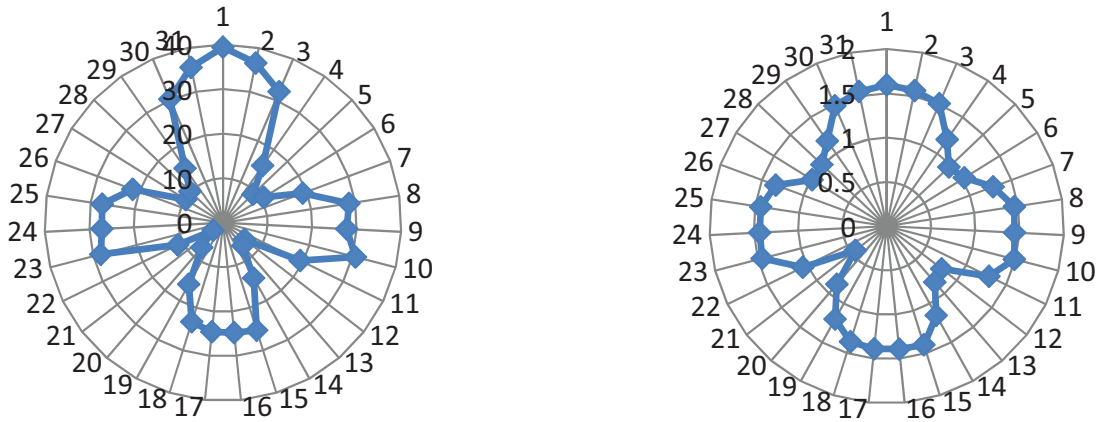


Figure 7. Polar plot over the vibration amplitude data pattern of Fig 6. Left: Linear scale. Right: Logarithmic scale.

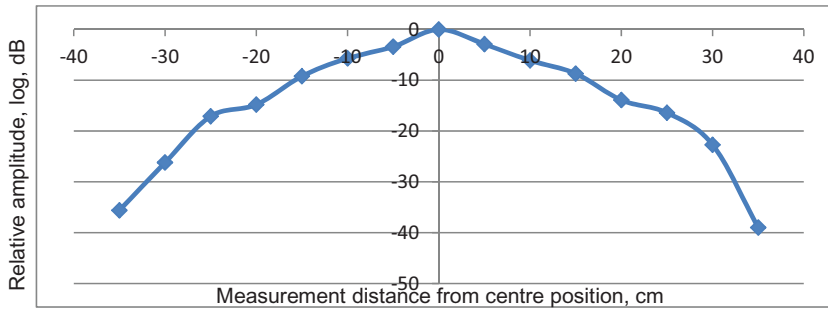


Figure 8. Relative vibration amplitude of the ovaling mode, in dB, as function of the lateral distance, in cm, from the point of application of the excitation force.

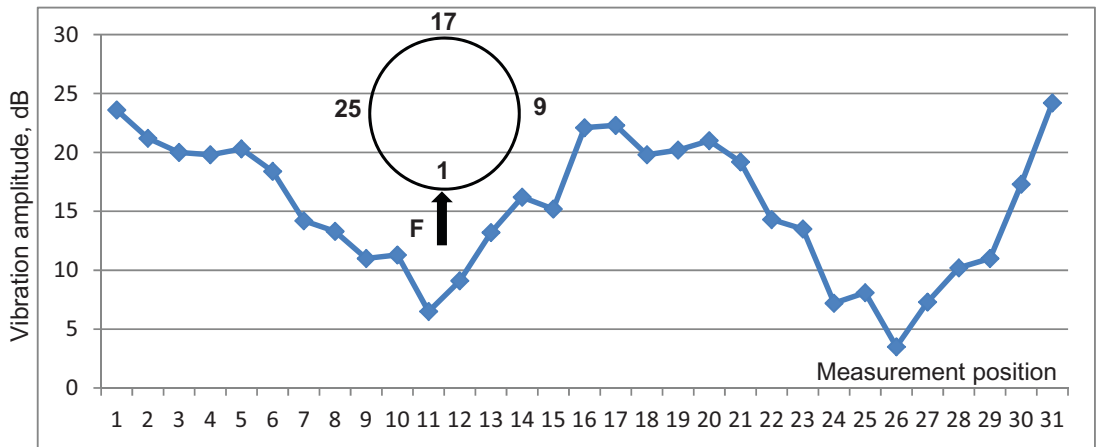


Figure 9. Vibration pattern along a circumference on the log for bending mode b1 at average frequency 190 Hz.

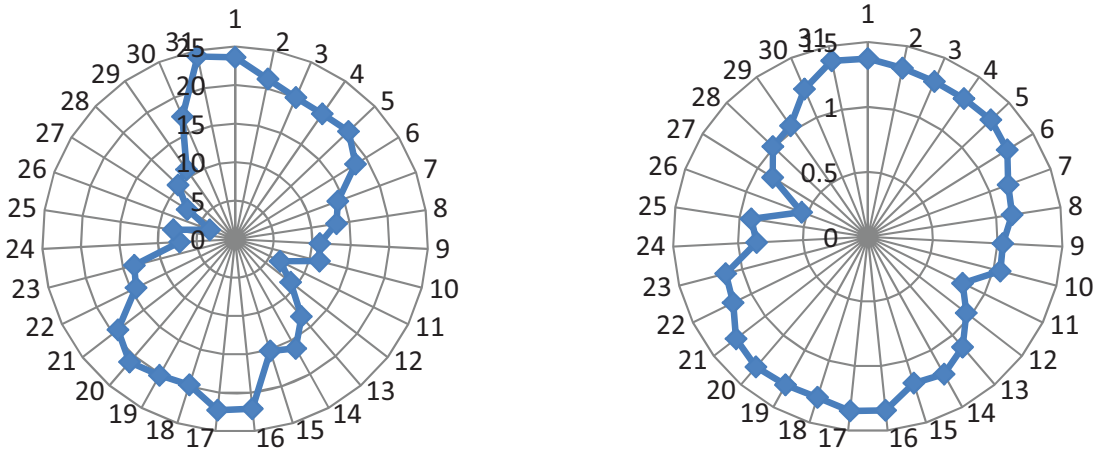


Figure 10. Polar plot over the vibration amplitude data pattern of Fig 9 for the first bending mode. Left: Linear scale. Right: Logarithmic scale.

modes. The excitation of these vibration modes depends primarily on the application position in the log of the force exciting source, the electrodynamic shaker, and on the orientation of the excitation force. For the purposes of this study the torsional and the longitudinal modes were excluded through attaching the rod fixed to the vibrating part of the shaker radially on the surface of the log and at mid-distance from its extremities. The choice of the position of the excitation force is also important inasmuch as the vibrational modes responding with their maximum amplitude will be those with such that an antinode line crosses the point of application of the excitation force. The surface jaggedness in the present experimental specimen hindered for some measurement points to be conducted at their prescribed position. The log also had some flaws on it and this caused disturbances for some measurements as it is known that flaws and delaminations are material defects that can cause modal coupling, not only enhancing the response of some modes and reducing that of others, but they even can generate new modes of vibration for the simple reason that their presence causes a change in the boundary conditions of the vibrational modes (Shen and Grady 1992).

The natural frequencies of a bar with large slenderness (ratio of length to width) of solid material

with MoE, E and density, ρ , and under flexural motion with free-free boundary conditions is expressed as (the approximation is often referred to as the Euler-Bernoulli, Cremer and Heckl 1988):

$$f_{f-f} = \frac{\pi}{8} \sqrt{\frac{B}{m}} \frac{(2n-1)^2}{l^2} \quad (1)$$

n being the number of nodes of the mode, and $B = EI$, the bending stiffness of the bar with I its sectional moment of inertia, which for a filled circular cylinder with radius a is expressed as:

$$I = \pi \frac{a^4}{2} \quad (2)$$

In Eq (1) m is the mass per unit length of the rod in kg/m; it is expressed as $m = \pi\rho Za^2$. The values of the natural frequencies of vibration for a bar of general dimensions are not expressible in as a simple explicit form as in Eq (1), but are instead determined through a nondirect procedure starting from the value of the slenderness of the bar and a frequency parameter. A system of equations is then established for the boundary conditions of the displacements of the beam's particles. From the latter the coefficients of the series' development leads to the values of the natural frequencies from setting the determinant of the

system of equations as equal to zero (Hutchinson 1980; Hutchinson 1981). The classical approximations underestimate the displacement and overestimate the natural frequencies of vibration as compared with results from more elaborated theories (starting from Timoshenko's in 1921; Sayyad 2011).

If we consider the first bending mode of a slender cylindrical beam, Eq (1) can be rearranged, with $n = 2$, as:

$$f_{f-f,1} = \frac{9\pi a}{8l^2} \sqrt{\frac{E}{2\rho}} \quad (3)$$

There are no exact available published data concerning the value of the MoE for the wood constituting the stem of date palm trees as opposed to those of other palm species. It is also important to mention that for trees, in general, the mechanical and strength properties of wood processed from their trunks depends on several parameters. These are not only limited to external growing conditions, like climatic and the chemical composition and water content properties of the soil on which the trees stand, but even on the part of the stem from which wood material is sawn. Regarding palm trees and due to the remarkable height, their size can reach up to 20-40 m, the MoE is found to be of distinctly higher values at the periphery of the stem and at its base. This mechanical characteristic enables these tall trees to withstand high strain constraints under windy conditions (Rich 1987; Gibson 2012). Using Eq (3) for the first bending resonance frequency $f_{f-f,1} = 170$ Hz gives a value for the MoE of $E = 63$ MPa (using a value of $490 \text{ kg}\cdot\text{m}^{-3}$ for its density as calculated from its weighing and measuring its volume). This value is noticeably low for softwood species (Douglas fir, Norway spruce, or oak), widely used as building materials, and which usually have values in the range 1-10 GPa, but it is also low as compared for lately reported MoE values of palms in the range 0.3-1.0 GPa (Rich 1987). Although these values apply for palm species other than the date. Because there were no visual signs of decay in the heart or near the periphery of the log under study, it is concluded that this

low MoE value, and if not what is expected from a date palm tree, may only be attributed to an aged palm tree from which the log was most probably cut, and which is supported by the large cross-sectional size, $\varnothing 45$ cm, of the test specimen. Moreover, it should be emphasized here that so far theoretical treatment concerns a slender beam, ie a beam whose length exceeds about 10 times its average cross-sectional size, and therefore a more elaborate approach is to be considered if a more accurate analysis is to be applied to present palm log. A further correction to be added to the analysis of thick beams is that of mass adding at the ends of the beam and which has for essential consequence to decrease the value of the resonance frequency of the vibration mode. This fact leads to an overestimate of the MOE, therefore the more qualitative than quantitative character of the present analysis.

The resonance frequency f_{cs} of the extensional vibrational modes is inversely proportional to the circumference C of the cylinder and directly dependent on the strength of the material filling the cylinder, especially on the propagation speed of shear waves v_s , ie $f_{cs} \approx xC^{-1}v_s$, x being a dimensionless factor proportional to the Poisson ratio of the material (Axmon et al 2002).

This pilot study is an incentive for the future, a more comprehensive and larger scale study needs to be conducted on the stem of standing palm trees. A recent publication by the author has shed some light on a method for extracting the ovalling mode from the frequency response of a palm tree trunk in response to a mechanical stress excitation. The method builds on using a combination of two similar vibration sensors attached to the trunk at two diametrically opposed positions and then to recording and adding their response (in phase) to the mechanical excitation induced radially at midway distance between the sensors (Ouis 2020). The tree specimen considered in that study was a California fan palm (*Washingtonia filifera*), and the results showed the possibility to determine the strength of the wood material at different heights above the ground from measuring the natural frequency of the ovalling mode as a function of the circumference of the trunk.

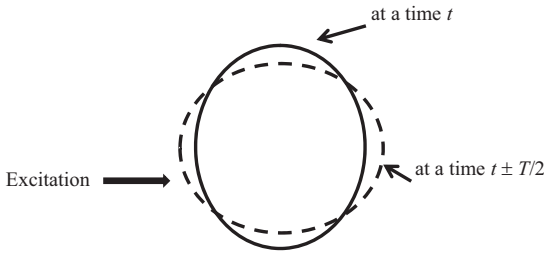
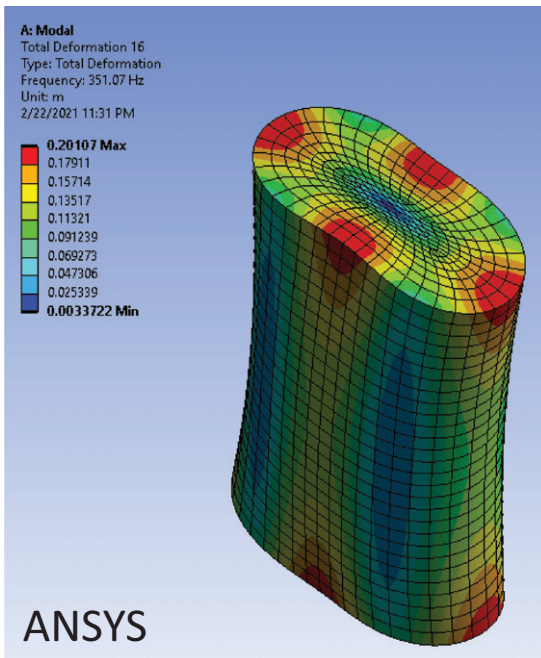


Figure 11. Illustration of the “ovalling” mode for a cylinder excited radially. T is the period of vibration of the mode, or $T = 1/f_{ov}$, f_o being its frequency.

The resonance frequency for a filled cylinder is proportional to the speed of wave propagation in the material, which in turn is proportional to the square root of the MOE. Hence a degradation of the strength of the cylinder material will result in a reduction of the value of the frequency of the ovalling mode, the vibration of which is illustrated in Figure 11. The aim of the present investigation is to serve as an initiator to a study at a

larger scale to be conducted on standing date palm trees of various sizes and planted on different stands to establish a possible correlation between the characteristics of the ovalling mode and the severity of rot attack in the tree stem.

Numerical calculations were conducted using mechanical and computational simulation Finite Element Analysis–based software. Two software, namely COMSOL Multiphysics and ANSYS, were used for predicting the shape and frequency of the ovalling mode of vibration on a cylinder with geometrical and physical attributes similar to those of the log used in this experimental study. A first computation with a cylinder made of isotropic material showed that for a value of MoE equal to 60 MPa, the frequency f_{ov} of the ovalling mode was obtained at 353 Hz. Including anisotropy in the material, specifically considering orthogonal isotropy between the radial and the axial directions, showed very minor effect on the value of f_{ov} ; with a Poisson ratio taken as 0.3, an



Eigenfrequency = 351.89 Hz.

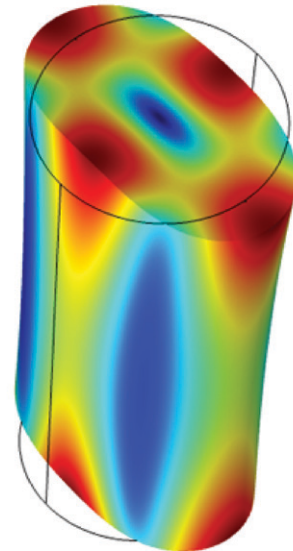


Figure 12. Numerical simulation and calculation of the vibration pattern and the frequency f_{ov} of the ovalling mode in a free solid cylinder made of material with orthogonal isotropy. Length $l = 1.10$ m, diameter $d = 0.45$ m, material density $\rho = 490$ kg/m³ and material stiffness MoE = 60 MPa. In both simulations the natural frequency of the mode was found $f_{ov} \approx 352$ Hz. Left: Using ANSYS. Right: using COMSOL Multiphysics.

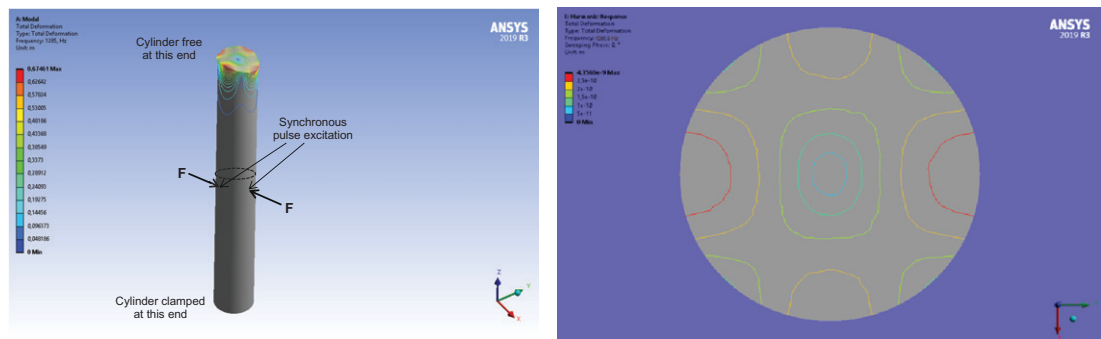


Figure 13. Left: Numerical simulation of the ovalling mode in a clamped-free solid isotropic cylinder subject to a pair of synchronous identical radial force pulses applied to its midst. Overall motion of the cylinder. Cylinder characteristics: height $h = 3.00$ m, diameter $d = 0.45$ m, material density $\rho = 490$ kg/m³ and material MoE = 750 MPa. Right: Details over the stress distribution on the cross section of the cylinder at a distance of 15.0 cm above the point of application of the excitation forces. Resonance frequency of the ovalling mode $f_{ov} = 1285$ Hz.

increase factor of 10 for the axial/tangential MOE resulted in a relative decrease of the f_{ov} by only 0.1%. (for palm trees' wood, the value of the MOE along the grain may be as high as 20 times that of the MOE value in the transverse direction). Figure 12 presents the results of calculations for this cylinder.

Assigning a value of 750 MPa for the tangential MOE resulted in a value of 1285 Hz for f_{ov} and this was taken for simulating, as a last investigation, the behavior of a filled cylinder with finite size and that was clamped, ie with no motion, at one end and free of motion at the other end (roughly representing the trunk of a standing tree). Its length was taken as 3.00 m for limiting the load and time of computations. The excitation of the cylinder was accomplished through the simultaneous application at midheight location on the cylinder of two similar force pulses radially opposed in direction and acting on two diametrically positions on the cylinder, Fig 13 (left). In the time domain, each of these force pulses was a half-sine shaped, with a maximum magnitude of 1.0×10^4 N, and a duration of 0.15 ms. The purpose of exciting the cylinder by two oppositely in-phase radial forces is to enhance the response of the ovalling mode (as well as that of all even cross-sectional modes). Figure 13 (left) illustrates the overall vibration of the cylinder, whereas on the right-hand side of the figure

is shown the deformation of its cross-sectional surface at a distance of 15.0 cm above the plane of application of the excitation forces (dotted line).

CONCLUSIONS AND FUTURE WORK

The objective from the investigation conducted in this study was to identify the vibrational modes that are excited in a palm tree trunk subject to a radial mechanical excitation and to study their attributes in terms of shape, frequency, and damping characteristics. Special emphasis was placed on the cross-sectional expansion "ovalling" mode, the vibration of which is considered as local as it is less affected by the axial extent of the tree trunk. From knowledge of the vibrational behavior and frequency of this particular mode, and which depends on the cross-size of the palm tree trunk, it may be possible to establish a correlation between the severity of rot attack in the trunk and the frequency of the ovalling mode.

ACKNOWLEDGMENTS

The author is much indebted to the Deanship of Scientific Research, DSR, at the King Fahd University of Petroleum & Minerals, KFUPM, for financing this research project, under project code IN141050 at the author's joining the

University. The submission of the final report to the research project has unwisely been delayed due to asynchronous availability of the test specimens and the measurement equipment. The latter has been provided through a loan from the Mechanical Engineering department at KFUPM, and for which Professor Y. Khulief is gratefully acknowledged.

REFERENCES

- Axmon J, Hansson M, Sornmo L (2002) Modal analysis of living spruce using a combined Prony and DFT multichannel method for detection of internal decay. *Mech Syst Signal Process* 16:561-584.
- Choi FC, Li L, Samali B, Crews K (2007) Application of modal-based damage-detection method to locate and evaluate damage in timber beams. *J Wood Sci* 53: 394-400.
- Cremer L, Heckl M (1988) *Structure borne sound*, 2nd edition. Springer Verlag, Berlin, Germany. https://books.google.com.sa/books?hl=en&lr=&id=5rPrCAAQBAJ&oi=fnd&pg=PR14&dq=Structure+Borne+Sound&ots=cF_UxLKgOm&sig=8MsqpiZNC9F7E0Z4MB2HJeQedJo&redir_esc=y#v=onepage&q=Structure%20Borne%20Sound&f=false.
- Deflorio G, Fink S, Schwarze F (2008) Detection of incipient decay in tree stems with sonic tomography after wounding and fungal inoculation. *Wood Sci Technol* 42:117-132.
- Gibson LJ (2012) The hierarchical structure and mechanics of plant materials. *J R Soc Interface* 9:2749-2766.
- Hutchinson JR (1980) Vibrations of solid cylinders. *J Appl Mech* 47:901-907.
- Hutchinson JR (1981) Transverse vibrations of beams, exact versus approximate solutions. *J Appl Mech* 48: 923-928.
- Kuttruff H (2010) *Room acoustics*, 5th edition. Elsevier Applied Science, London, United Kingdom.
- Mattheck CG, Bethge KA (1993) Detection of decay in trees with the Metriguard stress wave timer. *J Arboric* 19:374-378.
- Müller S, Massarani P (2001) Transfer-function measurement with sweeps. *J Audio Eng Soc* 49:443-471.
- Ouis D (2020) Monitoring of a cross-sectional vibrational mode in the trunk of a palm tree. *Arboric Urban For* 46(4):307-318.
- Rich PM (1987) Developmental anatomy of the stem of *Welfia geogii*, *Iriartea gigantea* and other arborescent palms: Implications for mechanical support. *Am J Bot* 74:792-802.
- Rust S (2000) A new tomographic device for the non-destructive testing of trees. Pages 233-237 in *Proc 12th International Symposium on Nondestructive Testing of Wood*, University of Western Hungary, Sopron, Hungary.
- Sayyad AS (2011) Comparison of various refined beam theories for the bending and free vibration analysis of thick beams. *Appl Comput Mech* 5:217-230.
- Schwarz BJ, Richardson MH (1999) *Experimental modal analysis*, CSI Reliability Week, Orlando, FL.
- Shen MH, Grady JE (1992) Free vibrations of delaminated beams. *AIAA J* 30:1361-1370.
- Wagener WW, Davidson RW (1954) Heart rots in living trees. *Bot Rev* 20:61-134.
- Yang X, Ishimaru Y, Iida I (2002) Application of modal analysis by transfer function to nondestructive testing of wood I: Determination of localized defects in wood by the shape of the flexural vibration wave. *J Wood Sci* 48:140-144.